Calculation of Profile Drag of Airfoils at Low Mach Numbers

TUNCER CEBECI* AND A. M. O. SMITH†
Douglas Aircraft Company, McDonnell Douglas Corporation, Long Beach, Calif.

This paper investigates the accuracy of a particular method for calculating the profile drag of airfoils at low Mach numbers. The method consists of 1) calculation of the pressure distribution by any suitable method, 2) calculation of laminar flow near the nose by Thwaites' method, 3) calculation of transition by Michel's method (if it is not known a priori), 4) calculation of turbulent boundary-layer flow by Head's method, and, finally, 5) calculation of momentum deficiency in the far wake by means of the Squire-Young relation. Profile drag has been calculated by this method for several airfoils at various angles of attack and Reynolds numbers. The effects of transition and airfoil thickness on the profile drag are studied. Comparison of calculated and experimental values show generally good agreement. The rms error based on 88 calculated drag values is 2.7%.

Nomenclature

c = chord length
C_D = section profile-drag coefficient
C_f = local skin-friction coefficient
C_l = section lift coefficient
H = shape factor, δ^*/θ
H_1 = shape factor, $(\delta - \delta^*)/\theta$
R_c = Reynolds number, $(u_\infty c)/\nu$
R_x = Reynolds number, $(u_e x)/\nu$
R_θ = Reynolds number, $(u_e\theta)/\nu$
t = airfoil-section thickness
u = x component of velocity
x = distance along body surface
α = angle of attack
δ = boundary-layer thickness
δ^* = displacement thickness
θ = momentum thickness
ν = kinematic viscosity

Subscripts

e = edge
L = lower surface
tr = transition point
U = upper surface
∞ = freestream

1. Introduction

IN the design of airfoils, an accurate calculation of the profile drag is essential, since this plays a very important role in the performance of an airplane. However, such a calculation is complicated by the fact that the profile drag depends not only on the section characteristics, but also on the degree and scale of turbulence in the free stream. Because the turbulence in most wind tunnels is not negligible, and because the scale of the turbulence is different from that in the atmosphere, it is difficult to predict, from model tests in a wind tunnel, the drag characteristics of an airfoil in flight in the comparatively turbulence-free atmosphere. The principal difficulty is the determination of the location of the transition point.

The purpose of this study is to evaluate a method of calculating the profile drag of an airfoil by means of a combination of existing boundary-layer methods, to compare the results with measurements obtained in low-turbulence wind tunnels, and thus to evaluate the accuracy of the method. The calculation procedure and the methods used to calculate the boundary-layer parameters are described in Sec. 2.

Received March 4, 1968; revision received May 27, 1968. The authors express their gratitude to George Mosinskis for performing many of the calculations in this study. This work was supported by the McDonnell Douglas Independent Research and Development (IRAD) program.

* Senior Engineer, Aerodynamics Research Group. Member AIAA.

† Assistant Chief of Aerodynamics for Research. Associate Fellow AIAA.

2. Procedure

The profile drag of an airfoil consists of skin friction due to tangential stresses at the surface and form drag due to the normal pressures. Skin-friction drag can be calculated with fair accuracy by boundary-layer theory. But the form drag, which is brought about by the boundary-layer displacement effect, in general cannot be calculated as accurately as skin-friction drag. For this reason, the profile drag of an airfoil is usually obtained by measurement. However, it can be calculated accurately if the development and behavior of the flow in the boundary layer and in the wake are known.

The flow along an airfoil can be divided into four regions. Consider the flow over the airfoil in Fig. 1. Starting at the forward stagnation point A, there is at first a region in which the flow is laminar. After a certain distance AB along the surface, which is dependent both on the pressure gradient along the surface and on the turbulence in the main stream, there is a region BC in which transition from laminar to turbulent flow takes place. In the third region, the flow from C to the trailing edge is fully turbulent. Finally, at the trailing edge D, the boundary layer of the upper surface joins that of the lower surface to form the turbulent wake. (Here, it is assumed that the boundary layer does not separate from the surface.)

A formula that is widely used in calculating the profile drag of an airfoil is the one developed by Squire and Young.[1] In order to use this formula, it is necessary to calculate the momentum thickness and the shape factor of the boundary layer at the trailing edge and also to know the velocity at the trailing edge. Determination of the boundary-layer parameters requires the following information: 1) the solution of the momentum equation in the laminar region, 2) the location of the transition region or the transition point, 3) the values of momentum thickness and shape factor in the transition region, 4) the solution of the momentum equation in the turbulent region.

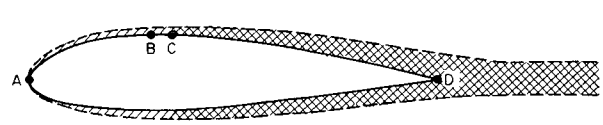

Fig. 1 Boundary-layer flow along an airfoil.

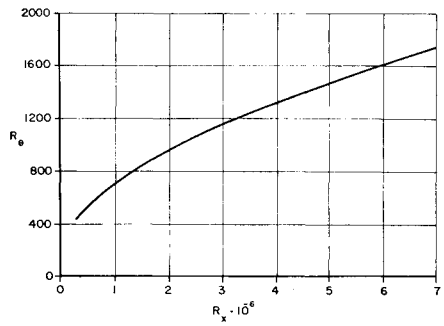

Fig. 2 Michel's transition-correlation curve.

In addition to these requirements, it is necessary to have the velocity distributions on the upper and the lower airfoil surfaces as basic data for the calculations, which can be obtained either experimentally or theoretically.

2.1 Laminar Region

The first step in profile-drag calculation is the determination of momentum thickness in the laminar region. There are several methods by which the momentum thickness can be determined; in this paper, Thwaites' method[2] is used. According to that method, the momentum thickness in the laminar region is calculated from

$$\frac{\theta}{c} = \left[\left(\frac{0.45}{R_c(u_e/u_\infty)^6}\right)\int_0^{x/c}\left(\frac{u_e}{u_\infty}\right)^5 d\left(\frac{x}{c}\right)\right]^{1/2} \tag{1}$$

Laminar separation takes place when

$$\frac{\theta}{c} = \left\{\frac{-0.090}{R_c[d(u/u_\infty)/d(x/c)]}\right\}^{1/2} \tag{2}$$

2.2 Transition Region

In order to calculate the profile drag, it is also necessary to know the region in which the boundary-layer flow changes from laminar to turbulent. The conditions of transition are determined by the velocity distribution, the Reynolds number, the degree of turbulence in the main stream, and the roughness and irregularities of the airfoil surface. Usually the chordwise distance over which transition occurs is small, so that transition may be considered to take place at a point.

The location of the transition point is generally determined by experiment. It may also be predicted by several empirical methods. The one used here is Michel's method,[3] which is based on a collection of experimental data on transition in which the downstream end of the region is taken as the transition point. This method, which uses a correlation curve (Fig. 2) in the R_θ, R_x plane, provides good results in locating the transition point, as long as the velocity distributions are smooth, the surface is smooth, and the turbulence low. The correlation curve can be represented by the following equation:

$$R_\theta \cdot 10^{-3} = C_1 R_x \cdot 10^{-6} + C_2 + [C_3(R_x \cdot 10^{-6})^2 + C_4 R_x \cdot 10^{-6} + C_5]^{1/2} \tag{3}$$

$$0.3 \cdot 10^6 \leqq R_x \leqq 7 \cdot 10^6$$

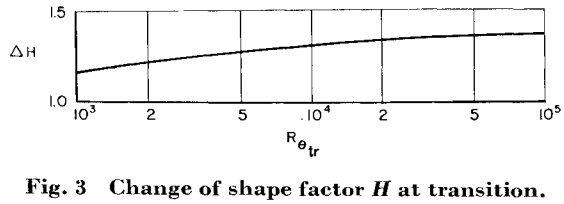

Fig. 3 Change of shape factor H at transition.

where

$$C_1 = -0.710 \qquad C_2 = -0.687 \qquad C_3 = 0.694$$
$$C_4 = 2.871 \qquad C_5 = 0.831$$

In the drag calculation reported here, Michel's transition correlation curve was used to locate the transition point when the experimental transition point was not given. If laminar separation takes place before the transition point is indicated by Michel's curve, the separation point is taken to be the transition point.

The momentum thickness was assumed to be continuous at the transition point; it was calculated from Eq. (1) and was taken as the initial value in the turbulent region. The initial value of the shape factor H in the turbulent region was obtained from Fig. 3, which is an empirical relationship given by Truckenbrodt on page 580 of Ref. 1. Here, $\Delta H = H_l(x_{tr}) - H_t(x_{tr})$, and $H_l(x_{tr})$ is obtained by Thwaites' method.

2.3 Turbulent Region

There are several methods for calculating the boundary-layer parameters in the turbulent region, but very few of them make use of the full equations of motion or of all of the well-established characteristics of the turbulent boundary layers, such as the law of the wall or the law of the wake. Recently, these approximate methods have been critically re-examined and, upon comparison, have been found to give widely different results.[4] Of these methods, Head's method was found to give better agreement with experiment than any of the other methods reviewed. For that reason, Head's method is used in this study. His method[5] uses the momentum integral equation

$$\frac{d\theta}{dx} + (H+2)\frac{\theta}{u_e}\frac{du_e}{dx} = \frac{C_f}{2} \tag{4}$$

and two auxiliary equations, namely, Ludwieg-Tillmann's expression for the skin-friction coefficient,

$$C_f = 0.246(10)^{-0.678H}(R_\theta)^{-0.268} \tag{5}$$

and a shape factor H obtained from the entrainment properties of the turbulent boundary layer. The latter is also related to another shape factor, H_1. The entrainment relation and shape-factor relations are as follows:

Entrainment relation:

$$(1/u_e)(d/d_x)(u_e\theta H_1) = 0.0299(H_1 - 3.0)^{-0.6169} \tag{6}$$

Shape-factor relation:

$$H_1 = G(H) \tag{7}$$

where

$$G(H) = \begin{cases} 0.8234(H-1.1)^{-1.287} & H \leqq 1.6 \\ 1.5501\,(H-0.6778)^{-3.064} + 3.3 & H \geqq 1.6 \end{cases}$$

2.4 Wake

In the wake, the skin friction vanishes, and hence the momentum equation there has the same form as Eq. (4) except that the right-hand side vanishes. Thus the equation is now integrable, and a practical approximation can be made that enables the profile-drag coefficient to be determined in terms of momentum thickness, shape factor, and velocity at the trailing edge. The relationship (for one surface) is shown in the Squire-Young formula[1]

$$C_D = 2(\theta/c)_{T.E.}(u_e/u_\infty)_{T.E.}^{0.5(H_{T.E.}+5)} \tag{8}$$

It is to be noted that the Squire-Young formula depends on the value of momentum thickness at the trailing edge as well as the value of the trailing-edge velocity, which is raised

to a power of about 3.2. If the experimental value of u_e/u_∞ is known, calculation of the drag presents no difficulty; however, if the theoretical inviscid potential-flow pressure distribution is to be used, then the Squire-Young formula is meaningless, since one will always get a stagnation point at the trailing edge (for finite trailing-edge angle). For this reason, a change was made in using Eq. (8); the values of velocity ratio, momentum-thickness ratio, and shape factor at the 95%-chord point were used, rather than the values at the trailing edge. The error arising from this approximation can be proved to be negligible by the analysis that follows.

In Ref. 6 [p. 182, Eq. (9)], the expression for the drag coefficient C_D for both laminar and turbulent flow is

$$C_D = \left[\frac{1.422}{R_c^{3/5}}\left\{\frac{u_{tr}}{u_\infty}\int_0^{x_{tr}/c}\left(\frac{u_e}{u_\infty}\right)^5 d\left(\frac{x}{c}\right)\right\}^{3/5} + \frac{0.02429}{R_c^{1/5}}\int_{x_{tr}/c}^1\left(\frac{u_e}{u_\infty}\right)^4 d\left(\frac{x}{c}\right)\right]^{5/6} \quad (9)$$

Now, consider only the contribution of the turbulent flow. Then

$$C_D = \left[\frac{0.02429}{R_c^{1/5}}\int_{x_{tr}/c}^1\left(\frac{u_e}{u_\infty}\right)^4 d(x/c)\right]^{5/6} \quad (10)$$

Assume that the velocity distribution between the 95%-chord point and the trailing edge is linear (Fig. 4). Then the velocity distribution is given by

$$u_e/u_\infty = a + 20(b - a)(x/c - 0.95) \quad 0.95 \leqq x/c \leqq 1 \quad (11)$$

where a is the value of the velocity at the 95%-chord point, and b is the value of the velocity at the trailing edge. Since Eq. (10) can be written as

$$C_D = \left[\frac{0.02429}{R_c^{1/5}}\int_{x_{tr}/c}^{0.95}\left(\frac{u_e}{u_\infty}\right)^4 d\left(\frac{x}{c}\right) + \frac{0.02429}{R_c^{1/5}}\int_{0.95}^1\left(\frac{u_e}{u_\infty}\right)^4 d\left(\frac{x}{c}\right)\right]^{5/6} \quad (12)$$

the term

$$C_{D_E} = \frac{0.02429}{R_c^{1/5}}\int_{0.95}^1\left(\frac{u_e}{u_\infty}\right)^4 d\left(\frac{x}{c}\right) \quad (13)$$

can be considered to be a "correction" or error term (assuming the exponent $\frac{5}{6} \approx 1$) when the profile drag is calculated at the 95%-chord point. Substituting the expression for the velocity ratio from Eq. (11) into Eq. (13) and integrating gives the correction or error term

$$C_{D_E} = (2.429/R_c^{1/5})10^{-4}(b^4 + ab^3 + a^2b^2 + a^3b + a^4) \quad (14a)$$

The preceding expression will be maximum when $b = a$.

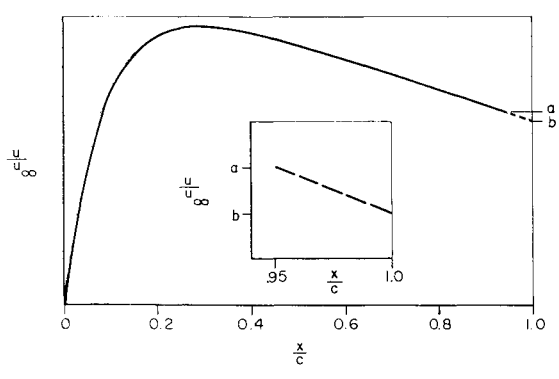

Fig. 4 Velocity distribution near the trailing edge.

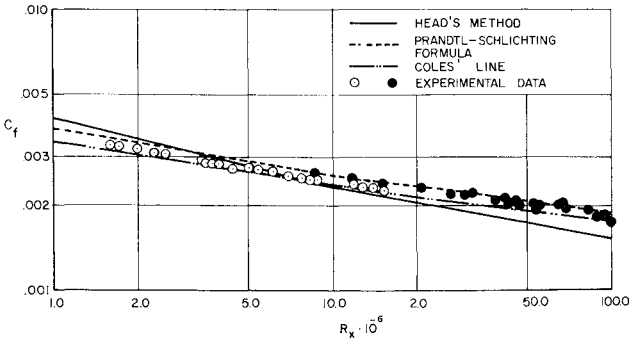

Fig. 5 Comparison of calculated local skin-friction coefficient with experiment, Prandtl-Schlichting formula, and Coles' line.

Then Eq. (14a) becomes

$$C_{D_E} = (5 \times 2.429/R_c^{1/5})10^{-4}a^4 \quad (14b)$$

If $a = 1$ and $R_c = 10^6$, the correction term is approximately 5×10^{-5}, which is relatively small. At higher chord Reynolds numbers, the correction term becomes even smaller. Thus, calculating the profile drag at values for the 95%-chord point, rather than for the trailing edge, is justified as a procedure for avoiding calculational difficulties very near the trailing edge.

3. Results

In order to investigate the accuracy of the procedure described in Sec. 2, profile drag was calculated for several airfoils at various angles of attack and Reynolds numbers for which experimental data are available. The calculated values were then compared with the experimental values. In general, it was found that the calculated drag values were consistently lower than the experimental drag values when the position of transition was calculated by Michel's method. For this reason, the calculated drag values (for cases where the position of transition was obtained by Michel's method) were plotted against the experimental values to determine an empirical constant that when multiplied by the calculated values would give a better agreement with experiment. The empirical constant, which was found to be 1.1, was used to multiply the momentum thickness calculated at the trailing edge when the position of transition was obtained by Michel's method. Thus, Eq. (8) becomes

$$C_D = 2[a\theta/c]_{T.E.}(u_e/u_\infty)^{0.5(H_{T.E.}+5)} \quad (15)$$

where $a = 1$ when transition is known experimentally and $a = 1.1$ when transition is calculated by Michel's method.

If $(u_e/u_\infty)_{T.E.}$ were to equal unity as on a flat plate, Eq. (15) should reduce to the well-known formula $C_D = 2(\theta/c)_{T.E.}$; Eq. (15) does not, because of the 1.1 factor. The factor can be considered to account for errors in the basic formulas for calculating θ/c, Sec. 2.1.

3.1 Comparison of Calculated and Experimental Profile-Drag Coefficients

In order to investigate the accuracy of Head's method, which is based on empirical correlations obtained at moderately low Reynolds numbers (maximum $R_\theta \approx 10{,}000$), the method was first used to calculate the local skin-friction coefficient on a flat plate as well as the profile-drag coefficients of three airfoils at high Reynolds numbers. The calculated results were then compared with the experimental and empirical results.

Figure 5 shows a comparison of local skin-friction coefficients calculated by Head's method and those calculated by

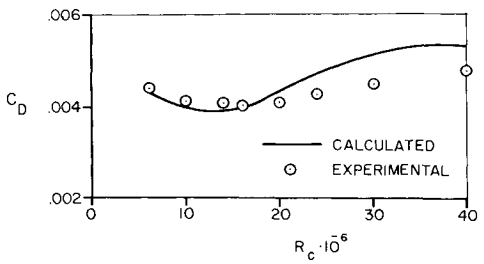

Fig. 6 Variation of profile-drag coefficient with Reynolds number for NACA $65_{(215)}$-114 airfoil. $C_l = 0.14$.

the Prandtl-Schlichting formula,[1]

$$C_f = (2 \log_{10} R_x - 0.65)^{-2.3} \tag{16}$$

as well as Coles' line,[7] which has been empirically fitted to experimental data. The flow was initially laminar, and the transition point was specified at $R_x = 1 \times 10^6$. Local skin-friction coefficients up to $R_x = 100 \times 10^6$ were calculated. The results indicate that the agreement up to $R_x = 10 \times 10^6$ (R_θ is about 13,000) seems to be satisfactory and that there is considerable deviation from the others only at higher Reynolds numbers.

Figure 6 shows the experimental profile-drag coefficients and the calculated profile-drag coefficients, together with the calculated transition points, of the NACA $65_{(215)}$-114 airfoil[8] for Reynolds numbers up to 40×10^6. The pressure distribution was calculated by Weber's method[9] for a lift coefficient of 0.14, and the transition points were determined by Michel's curve. The results indicate that the agreement up to $R_c = 20 \times 10^6$ is very good and that again there is considerable deviation from the experimental data at higher Reynolds numbers.

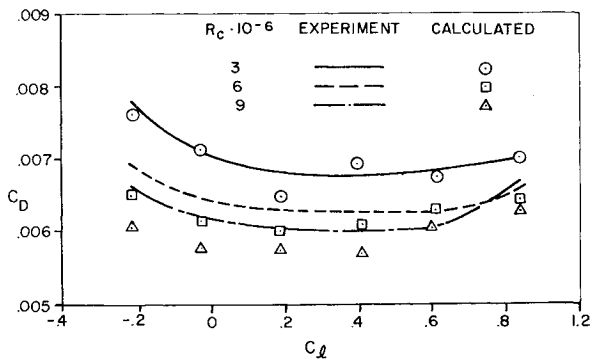

a) 4412 airfoil

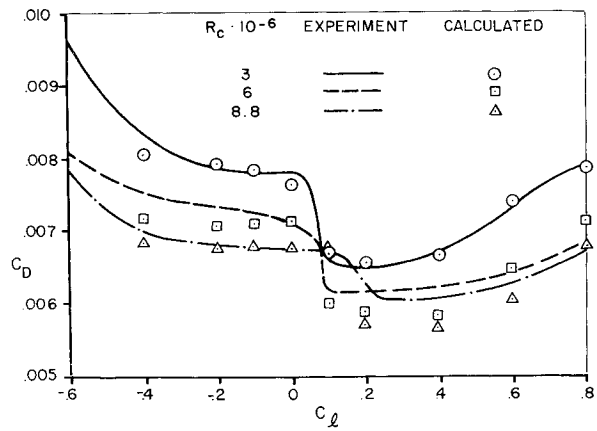

b) 23012 airfoil

Fig. 7 Calculated and experimental profile-drag coefficients of the NACA airfoil.

Table 1 Calculated and experimental profile-drag coefficients of the King Cobra airfoil

Reynolds number $R_c \times 10^{-6}$	C_l	Calculated transition point $(x/x)_U$	$(x/c)_L$	Calculated $C_D \times 10^3$	Experimental $C_D \times 10^3$
8	0.50	0.046	0.634	7.8	7.5
10	0.30	0.514	0.634	4.55	5.1
12	0.20	0.605	0.604	3.6	3.5

Table 1 shows a comparison of calculated profile-drag coefficients with the experimental values obtained in flight tests on the wing of the King Cobra aircraft.[10] The wing had an NACA 66-216 section at the tip; hence the maximum suction at the design lift coefficient was at the 60%-chord point, and the maximum thickness-chord ratio was nearly 16%. The profile drag was measured at a section 137 in. from the aircraft centerline. The experimental values in Table 1 were obtained when a test portion about 3 ft in span was very carefully treated to decrease the waviness of the surface. Considering the uncertainty in experimental data (for different flight conditions, the experimental drag values showed about 15% scatter), the calculated results are quite satisfactory.

The third airfoil whose profile drag was calculated at high Reynolds number was the NACA 35-215 airfoil. For this airfoil, the profile-drag coefficient of the upper surface was calculated for a pressure distribution obtained from Ref. 11 at a chord Reynolds number of 26.7×10^6. The experimental transition point was specified as the 43.5%-chord point. The calculated and the experimental (flight) values are 0.00232 and 0.00230, respectively.

The accuracy of calculating the profile-drag coefficient of airfoils by the formula given by Eq. (15) was extended to other airfoils for which the experimental drag data were available for chord Reynolds numbers between 3×10^6 and 9×10^6. Figure 7a shows the calculated and the experimental profile-drag coefficients[12] of the NACA 4412 airfoil for chord Reynolds numbers of 3, 6, and 9 million. The pressure distribution was obtained from the experiments of Ref. 13. The transition points were determined by Michel's curve. The calculations were limited to angles of attack between $-6°$ and $+6°$ because, according to Head's method, at higher angles of attack ($\alpha > 6°$) the flow separated. At an angle of 8°, the flow did not separate. However, the transition point for the pressure side could not be obtained by Michel's transition curve; that is, the flow was laminar from the leading edge to the trailing edge, and consequently profile drag for this side could not be calculated by Eq. (15). The agreement is best at the lowest Reynolds number, the one at which the experimental pressure distribution was obtained. The calculated values differ from the experimental values with increasing chord Reynolds number.

Figure 7b shows calculated and experimental profile-drag coefficients of the NACA 23012 airfoil at 3 chord Reynolds numbers for lift coefficients between -0.4 and $+0.8$. The pressure distribution was obtained by Weber's method, and the transition points were determined by Michel's curve. The agreement is good.

Figure 8 shows calculated and experimental profile-drag coefficients of the NACA 64-012, 64-212, and 64-412 airfoils for a chord Reynolds number of 9×10^6. The pressure distribution was obtained by Weber's method, and the transition points were determined by Michel's curve. Calculations were made for lift coefficients between -0.3 and $+0.6$. The agreement is good.

Figure 9 shows calculated and experimental profile-drag coefficients of the NACA 0012 airfoil for a chord Reynolds number of 6×10^6. The pressure distribution was obtained

Table 2 Calculated and experimental profile-drag coefficients of the symmetrical NACA four-digit airfoils

Airfoil	Calculated transition point x/c	Calculated $C_D \times 10^3$	Experimental $C_D \times 10^3$
0006	0.320	5.10	5.00
0009	0.336	5.75	5.50
0012	0.357	5.95	6.00
0018	0.362	6.35	...
0021	0.377	6.49	...

by Weber's method, and the transition points were determined by Michel's curve. The calculations were made for lift coefficients from -0.6 to $+0.6$. Figure 9 also shows the calculated values for $C_l = -0.16$, 0, and $+0.16$. The drag coefficients were calculated by Michel's curve and also for the experimental transition points given in Ref. 14. The transition points obtained from Michel's curve were consistently farther aft than the experimental transition points, which illustrates the need for a correlation constant, since late transition causes lower drag values.

Another airfoil considered was the NACA 4-006 airfoil, whose pressure distribution was obtained from Ref. 15. The chord Reynolds number was 3×10^6. The boundary layer was tripped at the 5%-chord point. The calculated and experimental values are both 0.008.

3.2 Effects of Transition and Airfoil Thickness on the Profile Drag

The study was extended to include the effects of transition and airfoil thickness on the profile drag of an airfoil. Symmetrical NACA four-digit airfoils with thicknesses from 6 to 21% were considered. At first, the transition point of each airfoil was determined by Michel's curve, and the zero-lift profile-drag coefficient was calculated by Eq. (15). Then the position of transition was varied from the leading edge to the 20%-chord point, and again the zero-lift profile-drag coefficients were calculated. In all cases, the pressure distributions given in Ref. 12 were used. The chord Reynolds number was taken as 6×10^6.

Table 2 shows the profile-drag coefficients calculated for the transition points determined by Michel's curve, together with the experimental values obtained from Ref. 12.

Figure 10 shows the calculated drag coefficients for two fixed transition points, namely, for $x/c = 0$ and $x/c = 0.20$, together with the results obtained by Hoerner's empirical equation,[16]

$$C_D/C_F = 2[1 + 2t/c + 60(t/c)^4] \qquad (17)$$

where C_F is the average skin-friction coefficient for a flat plate. Equation (17) is recommended for airfoil sections with maximum thickness located at or near the 30%-chord point and is therefore well suited to the NACA four-digit series. The skin-friction coefficient for the flat plate was calculated by the following formula, taken from Ref. 1.

$$C_F = 0.074/R_c^{0.20} - A/R_c \qquad 5 \times 10^5 < R_c < 10^7 \qquad (18)$$

where

$$A = R_{tr}(0.074/R_c^{0.20} - 1.328/R_{tr}^{0.5})$$

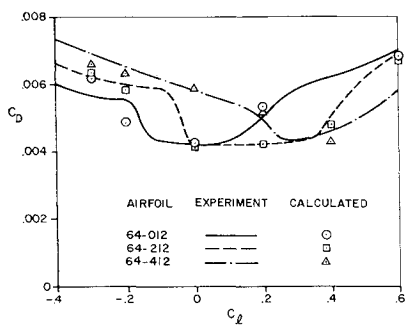

Fig. 8 Calculated and experimental profile-drag coefficient of the NACA 64-Series.

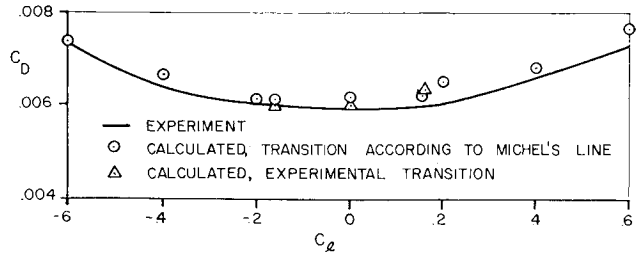

Fig. 9 Calculated and experimental profile-drag coefficients of the NACA 0012 airfoil. $R_c = 6 \times 10^6$.

3.3 Summary of Results

A method for calculating the profile drag of airfoils at low Mach numbers by the procedure described in Sec. 2 was investigated. Eighty-eight profile-drag values for several airfoils at various angles of attack and Reynolds number were calculated and compared with the experimental values. The results are summarized in Table 3 and in Fig. 11. Considering the various factors that influence the calculations, the results are good. Except for a few values, the maximum error is within $\pm 7\%$ and the rms error based on the 88 calculated drag values is 2.7%.

4. Discussion

Because of the many factors that affect the calculations, an accurate calculation of the profile drag of an airfoil is a very difficult matter. The most important of these factors is the position of transition. Since the profile drag, as given by the Squire-Young formula, is directly proportional to the momentum thickness at the trailing edge of the airfoil, it is necessary to calculate the momentum thickness as accurately as possible. Although none of the approximate calculation method uses the full equations of motion or all of the well-established characteristics of the turbulent boundary layers, some of them are quite satisfactory. Head's method is particularly well suited for typical flows over airfoils, namely, nonequilibrium and separating flows. This statement is supported by the extensive study reported in Ref. 4. Furthermore, any error in estimating the position of transition will affect the momentum thickness and consequently the profile drag.

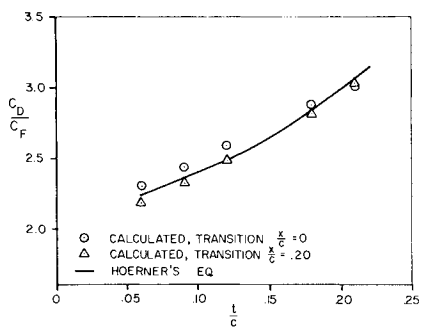

Fig. 10 Comparison of drag coefficients of symmetrical NACA four-digit airfoils calculated by the present method and by Horner's formula.

Table 3 Calculated and experimental profile-drag coefficients of the NACA $65_{(215)}$-114, King Cobra, NACA 35-215, NACA 4412, NACA 23012, NACA 64-series, NACA four-digit series, and NACA 4-006 airfoils

Airfoil	Reynolds Number $R_c \times 10^{-6}$	Angle of Incidence α deg	Lift Coefficient C_l	Calculated Transition Point $(\frac{x}{c})_U$	Calculated Transition Point $(\frac{x}{c})_L$	Profile-Drag Coefficient Calculated $C_D \times 10^3$	Profile-Drag Coefficient Experimental $C_D \times 10^3$	Reference	Test Facility
NACA 65 (215)-114	6		.14	0.54	0.54	4.40	4.40	8	NACA Low
	10		.14	0.54	0.54	3.90	4.10		Turbulence
	14		.14	0.49	0.54	3.85	4.05		
	16		.14	0.47	0.50	4.0	4.0		
	20		.14	0.40	0.44	4.35	4.10		
	24		.14	0.33	0.37	4.84	4.25		
	30		.14	0.31	0.31	5.0	4.50		
	40		.14	0.22	0.26	5.3	4.80		
King Cobra	8		.50	0.046	0.634	7.80	7.50	10	R. A. E.
	10		.30	0.514	0.634	4.55	5.10		Flight
	12		.20	0.604	0.604	3.60	3.50		Test
NACA 35-215	26.7			0.435[a]		2.32	2.30	11	NACA
NACA 4412	3	-6	-.211	0.747	0.028	7.61	7.80	12	Flight Test TDPT
		-4	-.0255	0.667	0.045	7.13	7.10		
		-2	.190	0.641	0.097	6.47	6.80		
		0	.410	0.484	0.144	6.93	6.75		
		2	.615	0.484	0.229	6.73	6.85		
		4	.840	0.364	0.539	7.00	7.00		
	6	-6	-.211	0.747	0.028	6.50	6.90		
		-4	-.0255	0.667	0.045	6.14	6.45		
		-2	.190	0.587	0.080	6.00	6.30		
		0	.410	0.484	0.110	6.09	6.25		
		2	.610	0.436	0.195	6.22	6.20		
		4	.840	0.340	0.458	6.41	6.60		
	9	-6	-.211	0.721	0.028	6.05	6.60		
		-4	-.0255	0.641	0.045	5.76	6.20		
		-2	.190	0.534	0.080	5.73	6.05		
		0	.410	0.484	0.093	5.67	6.00		
		2	.605	0.388	0.178	6.04	6.05		
		4	.840	0.316	0.357	6.26	6.70		
NACA 23012	3		-.4	0.661	0.031	8.05	8.30		
			-.2	0.483	0.062	7.92	7.85		
			-.1	0.425	0.098	7.84	7.75		
			0	0.358	0.20	7.62	7.75		
			.1	0.308	0.452	6.69	6.60		
			.2	0.266	0.570	6.55	6.50		
			.4	0.207	0.708	6.65	6.70		
			.6	0.166	0.721	7.38	7.30		
			.8	0.133	0.900	7.86	7.90		
	6		-.4	0.600	0.028	7.18	7.50		
			-.2	0.450	0.050	7.06	7.35		
			-.1	0.392	0.059	7.09	7.25		
			0	0.333	0.075	7.13	7 10		
			.1	0.283	0.422	6.00	6.15		
			.2	0.250	0.521	5.87	6.15		
			.4	0.186	0.708	5.83	6.20		
			.6	0.153	0.721	6.48	6.42		
			.8	0.107	0.900	7.15	6.85		

Table 3 (continued)

Airfoil	Reynolds Number $R_c \times 10^{-6}$	Angle of Incidence α deg	Lift Coefficient C_l	Calculated Transition Point $(\frac{x}{c})_U$	Calculated Transition Point $(\frac{x}{c})_L$	Profile-Drag Coefficient Calculated $C_D \times 10^3$	Profile-Drag Coefficient Experimental $C_D \times 10^3$	Reference	Test Facility
NACA 23012	8.8		-.4	0.541	0.028	6.83	7.00	12	NACA Flight Test
			-.2	0.425	0.037	6.74	6.80		TDPT
			-.1	0.358	0.046	6.78	6.75		
			0	0.316	0.059	6.76	6.75		
			.1	0.275	0.087	6.78	6.70		
			.2	0.233	0.462	5.70	6.25		
			.4	0.186	0.655	5.66	6.05		
			.6	0.143	0.721	6.05	6.25		
			.8	0.097	0.900	6.77	6.73		
NACA 64-012	9		-.3	0.59	0.09	6.19	5.8		
			-.2	0.59	0.32	4.84	5.5		
			0	0.50	0.50	4.21	4.2		
			.2	0.23	0.58	5.30	5.0		
			.4	0.09	0.60	6.10	6.2		
			.6	0.09	0.67	6.80	7.0		
NACA 64-212			-.3	0.68	0.046	6.35	6.2		
			-.2	0.64	0.09	5.86	6.0		
			0	0.60	0.14	4.10	4.2		
			.2	0.59	0.50	4.19	4.2		
			.4	0.37	0.59	4.77	5.0		
			.6	0.09	0.65	6.72	6.9		
NACA 64-412			-.3	0.73	0.046	6.60	6.9		
			-.2	0.68	0.046	6.32	6.5		
			0	0.65	0.046	5.85	5.8		
			.2	0.60	0.14	5.20	4.9		
			.4	0.51	0.50	4.27	4.5		
			.6	0.37	0.59	5.70	5.8		
NACA 0012	6		-.6	0.760	0.036	7.35	7.30		
			-.4	0.614	0.084	6.65	6.70		
			-.2	0.466	0.194	6.30	6.00		
			-.16	0.352[a]	0.20	5.95	5.95		
			0	0.265[a]	0.265	6.00	6.00		
			0	0.300	0.300[a]	6.10	6.00		
			.16	0.20	0.352[a]	5.95	5.95		
			.2	0.194	0.466	6.35	6.00		
			.4	0.084	0.614	6.80	6.70		
			.6	0.036	0.760	7.35	7.30		
NACA 4-006	3	0	-	0.05[a]	0.05[a]	8.00	8.00		
NACA 0006	6	0	-	0.32	0.32	5.10	5.00	12	TDPT
NACA 0009	6	0	-	0.336	0.336	5.75	5.50	12	TDPT

[a] Experimental Transition Points;
TDPT = Two-Dimensional Pressure Tunnel.

In the calculations reported here, the position of transition was obtained by Michel's transition-correlation curve. In almost all cases, the calculated profile-drag values were consistently lower than the experimental values. It was found that multiplication by an empirical constant gave better agreement. On the other hand, when experimental transition points were used, the agreement was good, and it was not necessary to use an empirical constant. This shows that in order to obtain a better agreement with experiment without using an empirical constant, it is necessary either 1) to specify the transition point or 2) to calculate the transition point by a method other than Michel's method. There are other empirical methods that can be used to calculate the transition point, but none of them is very satisfactory.

The results also show that calculation of the boundary-layer parameters, such as skin-friction coefficient and momentum thickness, is not very accurate at high Reynolds numbers. The calculated local skin-friction coefficients on a flat plate show considerable deviation from experimental values at Reynolds numbers R_θ greater than 13,000. The calculated profile-drag values also begin to deviate more from experimental values at higher Reynolds numbers. In

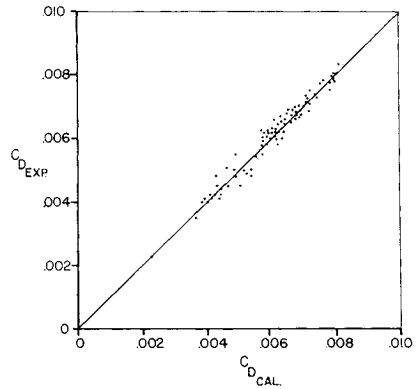

Fig. 11 Comparison of calculated profile-drag coefficients with experiment.

the latter case, the accuracy of calculating the profile drag at high Reynolds numbers is further complicated by the method used to calculate the momentum thickness and the shape factor, in addition to the method used to calculate the transition point.

The basic requirements for a good total method are accurate and rapid methods for the calculation of 1) laminar flow, 2) transition, 3) turbulent flow, and 4) the wake. The present choice of methods is by no means the only one. In fact, the one for turbulent flow is weak because it fails to predict flat-plate drag correctly at high Reynolds numbers. Fortunately, methods are on the horizon that should enable the turbulent boundary layer to be calculated accurately at very high Reynolds numbers. Nark[17] has recently reported on a method that is different in detail but similar in concept to the present one. He obtained essentially the same degree of accuracy. Nash and Osborne, in England, have also worked on the problem, with special attention to the effect of compressibility at subsonic speeds.[18–20] They too obtained about the same level of accuracy. The main accomplishment of the present paper therefore is to define one system of calculation and then evaluate it by a sufficient number of cases to give a meaningful assessment of its accuracy. The result, in turn, shows the state of the art on this important and very fundamental problem.

References

[1] Schlichting, H., *Boundary-Layer Theory*, McGraw Hill, New York, 1960.

[2] Thwaites, B., "Approximate Calculation of the Laminar Boundary Layer," *The Aeronautical Quarterly*, Nov. 1949.

[3] Smith, A. M. O. and Gamberoni, N., "Transition, Pressure Gradient and Stability Theory," Rept. ES 26388, Aug. 1956, Douglas Aircraft Co.

[4] Thompson, B. G. J., "A Critical Review of Existing Methods of Calculating the Turbulent Boundary Layer," 26 109 F.M.3492, Aug. 1964, Aeronautical Research Council, England.

[5] Head, M. R., "Entrainment in the Turbulent Boundary Layer," R and M 3152, 1960, Aeronautical Research Council, England.

[6] Thwaites, B., *Incompressible Aerodynamics*, Oxford University Press, Oxford, England, 1960.

[7] Coles, D., "Measurements in the Boundary Layer on a Smooth Flat Plate in Supersonic Flow. I. The Problem of the Turbulent Boundary Layer," Rept. 20-69, June 1953, Jet Propulsion Lab., Pasadena, Calif.

[8] Braslow, A. L. and Visconti, F., "Investigation of Boundary-Layer Reynolds Number for Transition on a NACA $65_{(215)}$-114 Airfoil in the Langley Two-Dimensional Low Turbulence Pressure Tunnel," TN 1704, 1948, NACA.

[9] Weber, J., "The Calculation of the Pressure Distribution on the Surface of Thick Cambered Wings and the Design of Wings with a Given Pressure Distribution," R and M 3026, 1957, Aeronautical Research Council, England.

[10] Smith, F. and Higton, D. J., "Flight Tests on 'King Cobra' FZ_{440} to Investigate the Practical Requirements for the Achievement of Low Profile-Drag Coefficients on a Low Drag Airfoil," R and M 2375, 1950, Aeronautical Research Council, England.

[11] Wetmore, J. W., Zalovcik, J. A., and Platt, R. C., "A Flight Investigation of the Boundary Layer Characteristics and Profile Drag of the NACA 35-215 Laminar Flow Airfoil at High Reynolds Numbers," Wartime Rept. L-532, May 1941, NACA.

[12] Abbott, I. H. and von Doenhoff, A. E., *Theory of Wing Sections*, Dover, New York, June 1958.

[13] Pinkerton, R., "Pressure Distributions over the Midspan Sections of the NACA 4412 Airfoil," Rept. 563, 1936, NACA.

[14] Becker, J. V., "Boundary Layer Transition on the NACA 0012 and 23012 Airfoils in the 8-Foot High Speed Wind Tunnel," Wartime Rept. L-682, Cl ACR, Jan. 1940, NACA.

[15] Paradiso, N. J., "Investigation at High and Low Subsonic Mach Numbers of Two Symmetrical 6-Percent-Thick Airfoil Sections Designed to Have High Maximum Lift Coefficients at Low Speeds," R and M L521-02, Oct. 1952, NACA.

[16] Hoerner, S. F., *Fluid-Dynamic Drag*, 3rd ed., published by author, 1965.

[17] Nark, T. C., "Theoretical Prediction of Airfoil Drag Polars," Paper presented at Society of Automotive Engineers Business Aircraft Meeting, April 3–5, 1968, Wichita, Kan.

[18] Nash, J. F., Moulden, T. H., and Osborne, J., "On the Variation of Profile Drag Coefficient below the Critical Mach Number," C.P. 758, Nov. 1963, Aeronautical Research Council, England.

[19] Nash, J. F., Osborne, J., and Macdonald, A. G. J., "A Note on the Prediction of Aerofoil Profile Drag at Subsonic Speeds," Aero. Rept. 1196, May 1966, National Physical Lab., England.

[20] Osborne, J., "The Variation of Profile Drag with Mach Number up to the Critical Value; a Comparison of Recent Predictions with Early Flight and Wind-Tunnel Measurements, and a Comment on an Earlier Prediction," Aero. Rept. 1197, June 1966, National Physical Lab., England.